Electronic Supplementary Material (ESI) for Journal of Materials Chemistry C.

Supporting Information

Manipulation of dual fluorescence behavior in aggregation-induced emission enhancement of a tetraphenylethene-appended polymer by optical tweezers

Shun-Fa Wang, Bo-Wei Chen, Ayami Itagaki, Fumitaka Ishiwari, Takanori Fukushima, Hiroshi Masuhara, and Teruki Sugiyama*

SI 1. Synthesis of the $pTPE_{0.01}$

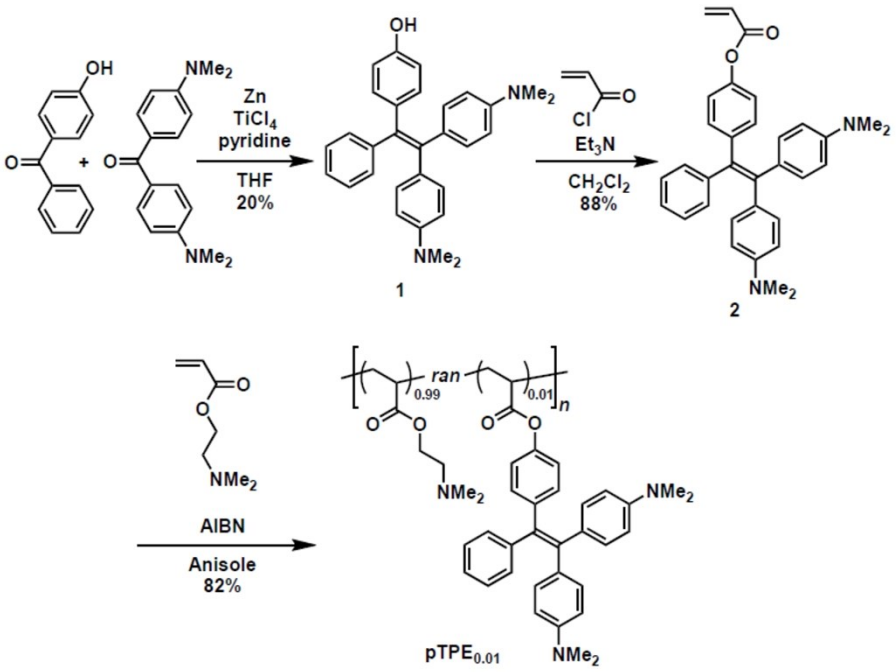

Figure S1. Synthetic scheme of $pTPE_{0.01}$

Materials;

Unless otherwise stated, chemical reagents were purchased from Sigma-Aldrich, TCI, and FUJIFILM Wako Pure Chemical Industries, Ltd. and used as received.

General;

NMR spectra were recorded at 25 °C on a Bruker model AVANCE-400 spectrometer (400.0 MHz for ^{1}H and 100.6 MHz for ^{13}C), where chemical shifts (δ) were determined with respect to residual non-deuterated solvent for ^{1}H ($CDCl_3$: $^{1}H(\delta)$ = 7.26 ppm), residual solvent for ^{13}C ($CDCl_3$: $^{13}C(\delta)$ = 78.0 ppm, CD_2Cl_2: $^{13}C(\delta)$ = 53.2 ppm). The absolute values of the coupling constants are given in Hertz (Hz), regardless of their signs. Multiplicities are abbreviated as singlet (s), doublet (d), multiplet (m) and broad (br). IR spectra were recorded at 25 °C on a JASCO model FT/IR-660$_{Plus}$ Fourier transform infrared spectrometer. High-resolution (HR) APCI-TOF mass spectrometry measurements were performed on a Bruker microTOF II mass spectrometer equipped with an atmospheric pressure chemical ionization (APCI) probe. Analytical size-exclusion chromatography (SEC) was performed at 40 °C regulated by column oven (CO-2065$_{Plus}$) on a JASCO HSS-1500 system equipped with a refraction index (RI) detector (RI-2031$_{Plus}$), using dimethylformamide (DMF) containing LiBr (0.01 M) as an eluent at a flow rate of 0.80 mL/min on a column (TSKgel 3000, TOSOH). The molecular weight calibration curve was obtained by using standard polystyrenes (TSKstandard polystyrene, TOSOH).

Synthesis of 4-hydroxy-4',4''-dimethylaminotetraphenylethene (1).

Under argon, $TiCl_4$ (2.75 mL, 25.0 mmol, 5 eq.) was slowly added to a THF (60 mL) suspension of zinc powder (3.25 g, 50.0 mmol) at 0 °C. The suspension was stirred at 25 °C for 30 min and refluxed for 2.5 h, and cooled again to 0 °C. After the addition of pyridine (1.00 mL, 12.5 mmol), the mixture was continuously stirred for 10 min. To the mixture, a THF (30 mL) solution of a mixture of 4-hydroxybenzophenone (0.990 g, 5.00 mmol) and 4,4'-bis(dimethylamino)benzophenone (1.34 g, 5.00 mmol) was slowly added, and the resultant mixture was stirred under reflux for 12 h and allowed to cool to 25 °C. After the addition of 10% K_2CO_3 aq. (50 mL), the reaction mixture was extracted with CH_2Cl_2. An organic phase separated was washed with water and brine, dried over $MgSO_4$, and then evaporated to dryness under reduced pressure. The residue was subjected to column chromatography on SiO_2 (CH_2Cl_2/MeOH; v/v = 95/5) to allow isolation of **1** as yellow-green solid (434 mg) in 20% yield: ^{1}H NMR (400 MHz, $CDCl_3$): δ (ppm) 7.02–7.18 (m, 5H), 6.87–6.96 (m, 6H), 6.56–6.45 (m, 6H), 5.26 (s, 1H), 2.89 (s, 12H). ^{13}C NMR (100 MHz, $CDCl_3$): δ (ppm) 40.5, 40.6, 111.6, 111.8, 114.6, 125.5, 127.5, 131.5, 132.4, 132.7, 136.8, 137.6, 140.4, 145.3, 148.7, 153.5. FT-IR (KBr): ν (cm^{-1}) 3429, 3029, 2889, 2880, 1608, 1519, 1479, 1442, 1352, 1261, 1225, 1193, 1168, 1124, 1100, 1069, 947, 817, 767, 751, 741, 701, 570. HRMS (APCI): calcd for $C_{30}H_{30}N_2O$ $[M]^+$: 434.2353; found: 434.2371. Analytical data (^{1}H and ^{13}C NMR spectra, FT-IR spectra, and high-resolution APCI-TOF mass spectra) of **1** are shown in Figures S12–S15.

Synthesis of 4-acryloyloxy-4',4''-dimethylaminotetraphenylethene (2).

Acryloyl chloride (16.0 μL, 200 μmol) was dropwise added at 0 °C to a CH_2Cl_2 solution (0.5 mL) of a mixture of **1** (43.4 mg, 100 μmol) and triethylamine (56.0 μL, 400 μmol). The resultant mixture was stirred at 25 °C for 12 h and then evaporated to dryness under reduced pressure. The residue was subjected to column chromatography on SiO_2 ($CHCl_3$/MeOH; v/v = 99/1) to allow isolation of **2** as yellow solid (42.7 mg) in 88% yield: ^{1}H NMR (400 MHz, $CDCl_3$): δ (ppm) 7.03–7.26 (m, 7H), 6.87–6.91 (m, 6H), 6.56 (dd, J = 17.3, 1.3 Hz, 1H), 6.47 (d, J = 9.0 Hz, 2H), 6.45 (d, J = 9.0 Hz, 2H), 6.28 (dd, J = 17.3, 10.4 Hz, 1H), 5.96 (dd, J = 10.4, 1.3 Hz, 1H), 2.90 (s, 6H), 2.88 (s, 6H) ppm. ^{13}C NMR (100 MHz, CD_2Cl_2) δ (ppm) 164.1, 148.9, 148.8, 148.2, 144.9, 142.7, 141.6, 135.6, 132.1, 132.4, 131.9, 131.8, 131.2, 127.8, 127.4, 125.4, 120.3, 111.0, 110.9, 39.9. FT-IR (KBr): ν (cm^{-1}) 3449, 3083, 3035, 2921, 2889, 2802, 1746, 1608, 1519, 1444, 1402, 1354, 1294, 1248, 1198, 1166, 1153, 1126, 1065, 1018, 976, 946, 902, 818, 768, 739, 700, 589, 471, 454, 432, 420. HRMS (APCI): calcd for $C_{33}H_{32}N_2O_2$ [M$^+$]: 488.2437; found: 488.2458. Analytical data (^{1}H and ^{13}C NMR spectra, FT-IR spectra, and high-resolution APCI-TOF mass spectra) of **2** are shown in Figures S16–S19.

Synthesis of $pTPE_{0.01}$.

An anisole solution (1.27 mL) of a mixture of **2** (9.8 mg, 0.021 mmol), 2-(dimethylamino)ethyl acrylate (302 μL, 1.99 mmol) and AIBN (1.7 mg, 0.01 μmol) was degassed by freeze-pump-thaw cycles (three times) and purged with argon. The mixture was stirred at 65 °C for 24 h and then allowed to cool to 25 °C. The reaction mixture was poured into *n*-hexane, and the precipitate formed was collected by decantation and dried under reduced pressure to afford $pTPE_{0.01}$ (71% yield) as slightly yellow powder (201 mg, 1.40 mmol for the monomer unit): ^{1}H NMR (400 MHz, $CDCl_3$): δ (ppm) 7.06–7.04 (m, 0.025H), 6.93–6.90 (m, 0.03H), 6.49–6.47 (m, 0.03H), 4.19 (br, 2H), 2.58 (br, 2H), 2.39 (br), 2.31 (s, 6H), 1.97 (br), 1.70 (br). FT-IR (KBr): ν (cm^{-1}) 3609, 3427, 2948, 2862, 2821, 2770, 1732, 1457, 1398, 1362, 1333, 1272, 1238, 1147, 1100, 1059, 1042, 1016, 966, 854, 779, 748, 532, 490, 451, 421. M_n = 13.4 kg mol^{-1}; M_w/M_n = 2.44 (SEC; based on polystyrene standards). Analytical data (^{1}H NMR and FT-IR spectra, and SEC trace) of **2** are shown in Figures S20–S22.

SI 2. Sample preparation for trapping experiments

We used a dye-appended polymer $pTPE_{0.01}$ (molecular weight: 13400 g/mol; polydispersity index: 2.44) composed of a linearly polymeric chain poly[2-(dimethylamino)ethyl acrylate] and a tertiary tetraphenylethene (TPE) substituent (1 %

composition; position at a random unit) as our target compound for trapping experiments. The $pTPE_{0.01}$ polymer was dissolved in a phosphate D_2O buffer solution (sodium dihydrogen phosphate-phosphoric acid in D_2O, 10 mM, pD = 2.6), and the concentration of the polymer solution was fixed to be 36 μM. Under our prepared condition, the polymer carried protonated charges at dimethylamino groups. D_2O (Sigma-Aldrich, 99.9%) was used as a solvent instead of H_2O to suppress local temperature elevation caused by laser heating under 1064-nm irradiation. The pD value was measured by adding 0.4 to a value measured by a pH meter (Mettler Toledo, F20-standard). The sample solution was stored in a glass bottle covered with aluminum foil and was stirred with a magnet bar at a rotation rate of 650 rpm overnight. The sample solution of 10 μL was injected into a hand-made glass container that was pretreated with an alkaline detergent solution in 10-time-dilution (Hellma Analytics, Hellmanex III), and soon a solution film in a thickness of 100–110 μm was prepared on the glass surface. The container with the solution was sealed with a glass slide that pasted grease to reduce solution evaporation during laser irradiation. The container was then placed on the stage of an inverted microscope (Olympus, IX-71) for laser irradiation.

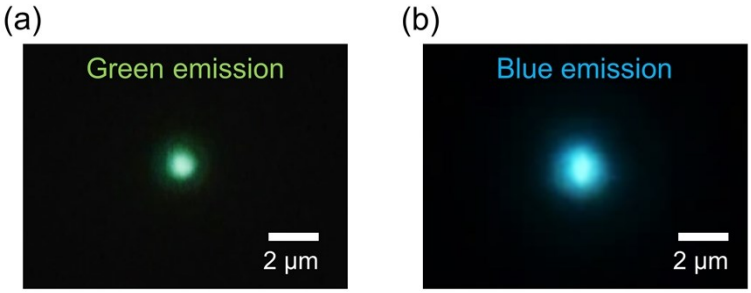

Figure S2. Enlarged fluorescence images from panels (iv) and (v) in Figure 1b, showing (a) green and (b) blue fluorescence emissions.

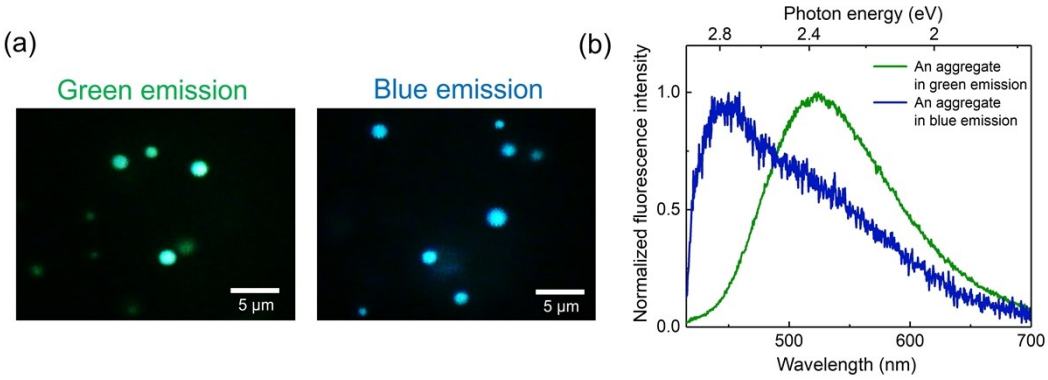

Figure S3. (a) The fluorescence image of aggregates of $pTPE_{0.01}$ polymer prepared at pD values of 7.1 (green emission) and 13.7 (blue emission) by deprotonation method, and their (b) normalized fluorescence spectrum. Their fluorescence peak positions were

around 525 and 445 nm, individually. The deprotonation method was conducted by pouring a small amount of concentrated NaOH solution (1 M) into the polymer solution of 2.5 mL in a 10-mm quartz cuvette cell. The poured alkaline solution neutralized the protonated polymer, triggering aggregation that led to the AIEE phenomenon. The formed fluorescent aggregates in micrometer size were seen with fluorescence microscopic images, and their fluorescence emissions were measured with the confocal microspectroscopy under excitation at 405 nm.

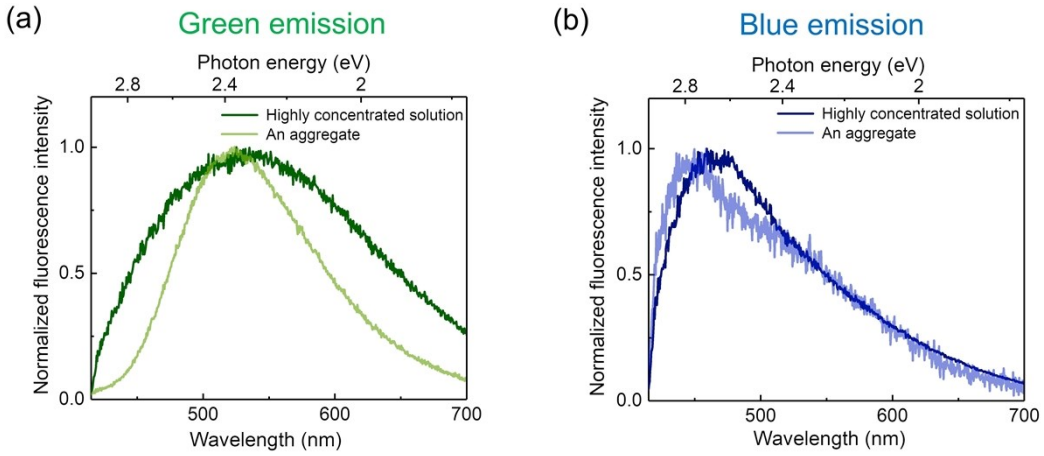

Figure S4. The fluorescence emissions of the highly concentrated solutions at trapping laser power of 20 (green emission) and 700 mW (blue emission) were compared with those of the fluorescent aggregates prepared at pD values of (a) 7.1 and (b) 13.7 by the deprotonation method. The highly concentrated solution in green emission showed broader fluorescence bandwidth than the aggregate. Such broad bandwidth implies wide conformation distribution of the polymer in the solution, probably caused by the conformational relaxation at the low laser power.

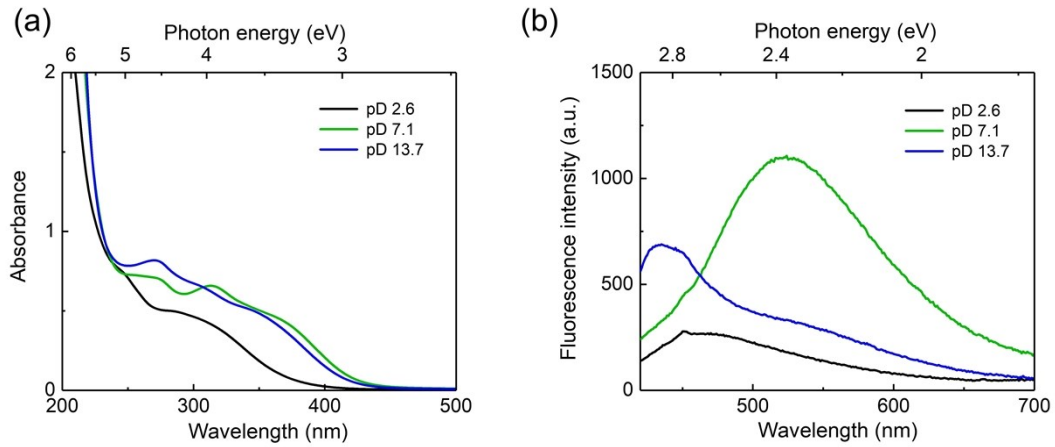

Figure S5. (a) Extinction spectrum of $pTPE_{0.01}$ bulk solution at different pD values, and (b) its fluorescence spectrum under the same pD conditions. These spectra were measured with a UV-Vis spectrophotometer (JASCO, V-670) and spectrofluorometer

(HORIBA, FluoroMax-4), respectively. The polymer solution at pD 2.6 shows almost no extinction in the visible wavelength region, whereas those at higher pD values show intensity increase in extinction in the wavelength below 450 nm. The extinction increment was caused by both reasons of light scattering from the micrometer-sized polymer aggregates and of n–π^* absorption of the lone pair electrons at the dimethylamino groups. Furthermore, the polymer solutions at higher pD values exhibit significant increases in fluorescence, and the peak position is 530 and 435 nm.

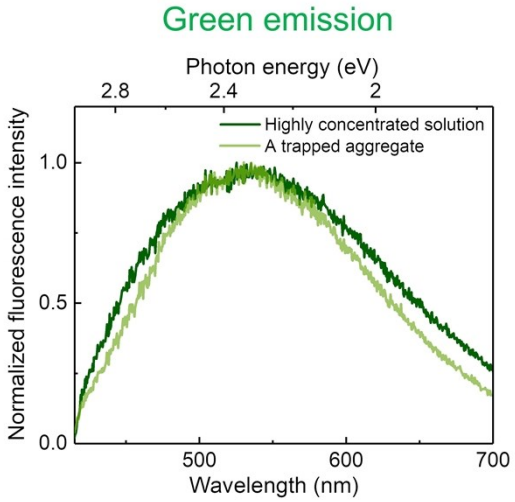

Figure S6. Normalized fluorescence spectrum of the highly concentrated solution and of a single aggregate by optical trapping at 20 and 700 mW, individually. Exposure time of each spectral frame is 3 s.

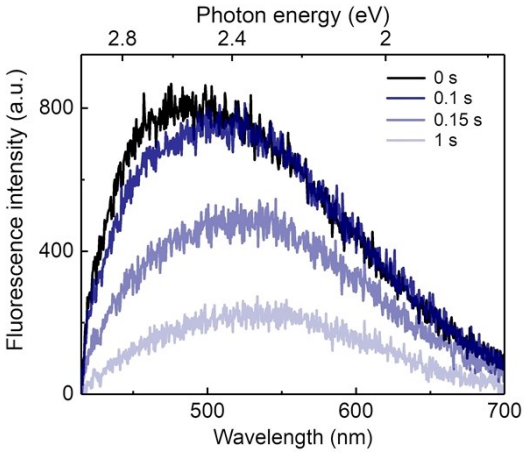

Figure S7. Fluorescence spectral change upon stopping trapping laser irradiation in the highly concentrated solution. The spectrum became flat at 3 s approximately after switching off the laser. The exposure time of each spectral frame is 0.05 s.

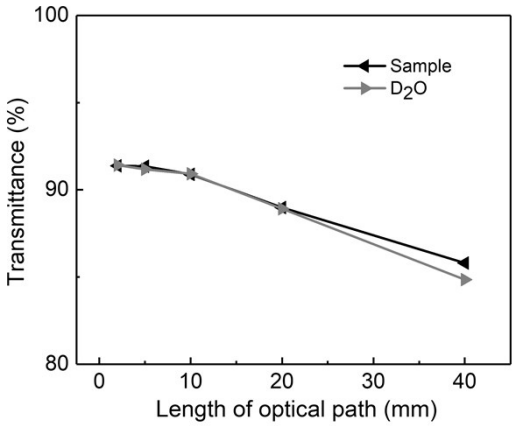

Figure S8. Transmittance of the $pTPE_{0.01}$ bulk solution and D_2O at 1064 nm as a function of the optical path length of a cuvette. Their transmittance at each path length shows no apparent difference. As reported by Ito et al., temperature elevation in D_2O at the focus of 1064-nm laser was estimated to be 2.6 K/W, and their experimental condition is similar to ours.[1] Thus, we could calculate the elevation degree in temperature for our sample solution by assuming its absorption same as D_2O, and the calculated value was 2 K approximately by the laser irradiation at 700 mW.

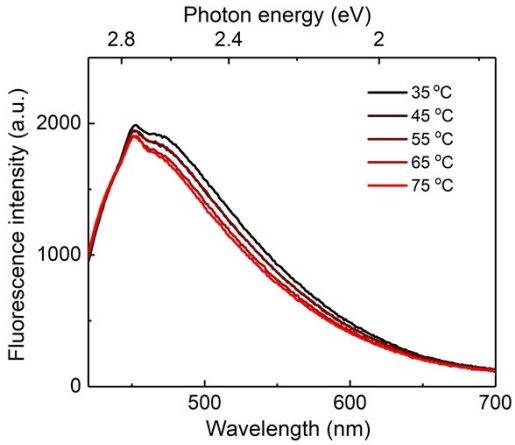

Figure S9. Fluorescence spectrum of the $pTPE_{0.01}$ bulk solution in temperature conditions ranging from 35 to 75 ℃. A small Raman peak at 450 nm was seen due to OD stretching (around 2500 cm^{-1}) of D_2O excited at 405 nm.

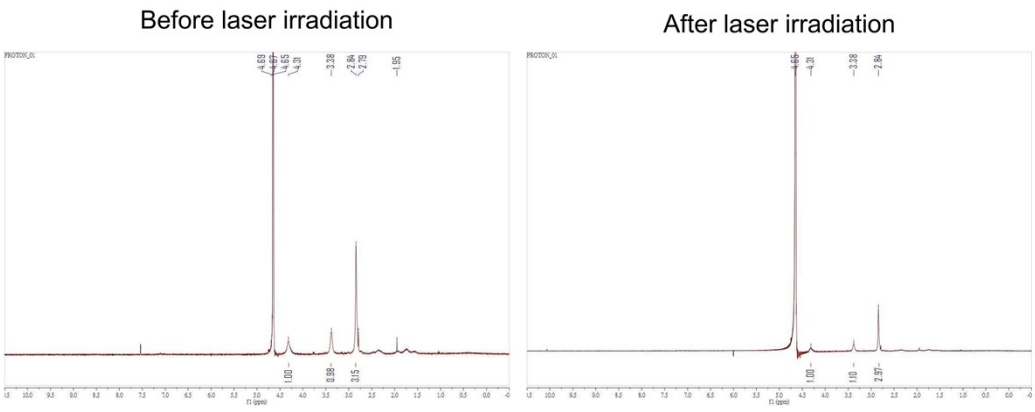

Figure S10. Nuclear magnetic resonance (NMR) spectrum of the $pTPE_{0.01}$ bulk solution (D_2O) and that after trapping laser irradiation by 30 min. The chemical shift and ratio of each peak were marked at the top and bottom sides of the spectrum. The NMR spectroscopic measurement was carried out by a spectrometer (Agilent, 400-MR DD2).

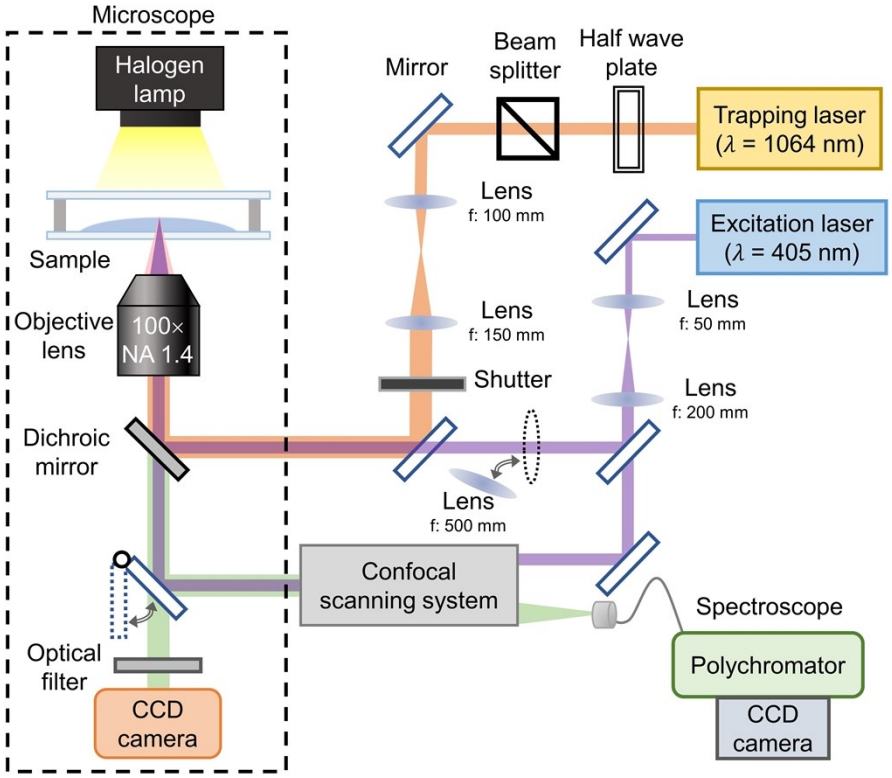

Figure S11. Schematic illustration of the optical setup for trapping experiments. A continuous-wave beam from a near-infrared 1064-nm laser (Laser Quantum, Ventus 1064) was used as a trapping light source. The laser beam was expanded in radial size by a beam collimator composed of two convex lenses with different focal lengths (f =

100 mm and 150 mm). The collimated beam was focused at the top surface of the solution through an oil-immersion objective lens (Olympus, 100×, NA = 1.40) on an inverted microscope (Olympus, IX-71). The laser power after the objective lens was tuned to 700 mW (100 MW/cm^2) for the trapping experiment. Except for the fixed power, the power was automatically controlled by changing the rotation angle of a half-wave plate in front of a beam splitter. The laser irradiation could be immediately cut off by a mechanical shutter (Shutter instrument, Lambda SC; close time: 8 ms). Optical trapping dynamics in laser irradiation were visualized in two manners with a charge-couple device (CCD) camera (Watec, WAT 231S2). One manner was transmission image obtained by white light illumination from a halogen lamp (Olympus, U-LH1001R). Another was a fluorescence image which required an excitation light source from a diode laser (Cobolt, MLD 405) at 405 nm for illumination. The effective size of the illumination was 1 μm or 45 μm, when the excitation light was tightly focused or widely illuminated through an additional lens (f = 500 mm). Throughout the objective lens, their power was measured to be 2.0 μW (2.0×10^3 W/cm^2) or 10 μW (0.7 W/cm^2), individually. Except for the image, fluorescence spectral change in during optical trapping was derived with a confocal microspectroscope. The fluorescence passed a confocal scanning system (Olympus, FV-300) and then was diffracted with a polychromator (Princeton Instruments, ACTON Spectra Pro 2300i) and was detected with a CCD detector (Princeton Instruments, PIXIS 400). The detection size was constrained to one μm in diameter approximately with a confocal pinhole. The confocal scanning system enabled the shift of the excitation light to various focal positions in two-dimension by controlling Galvano mirrors while keeping the same laser power at those positions. All the trapping experiments were carried out at room temperature (25℃).

Analytical Data

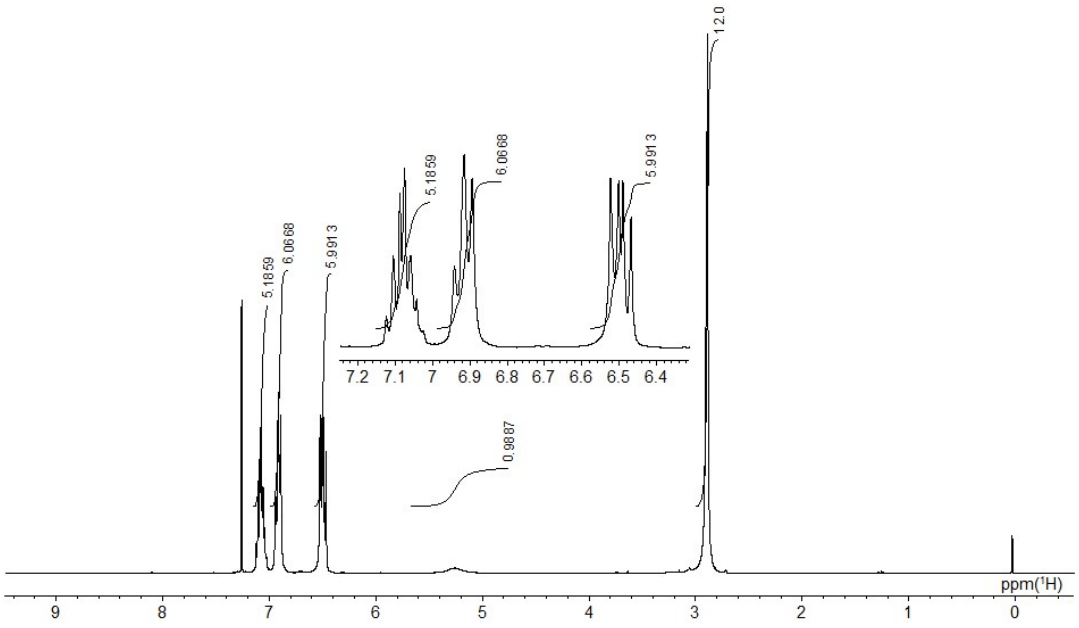

Figure S12. ^{1}H NMR spectrum (400 MHz) of **1** in $CDCl_3$ at 25 °C.

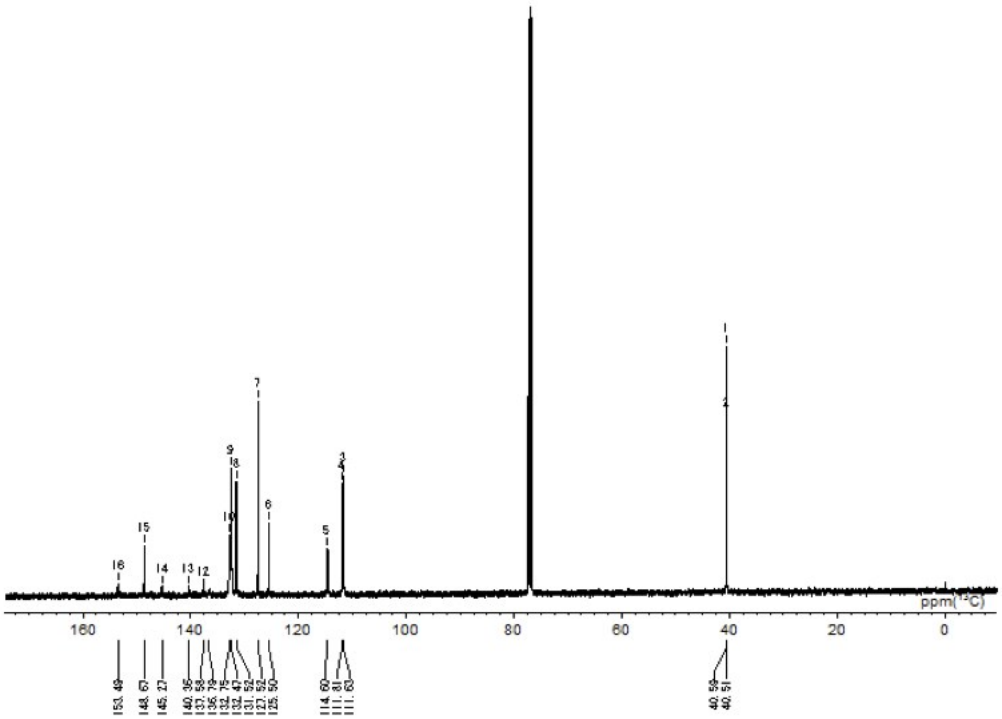

Figure S13. ^{13}C NMR spectrum (100 MHz) of **1** in $CDCl_3$ at 25 °C.

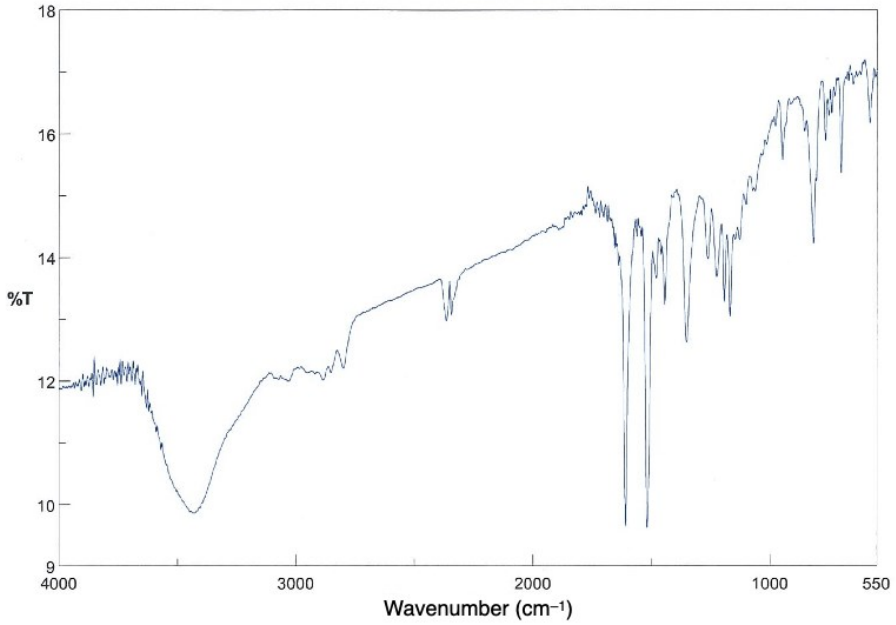

Figure S14. FT-IR spectrum of **1** at 25 °C (KBr).

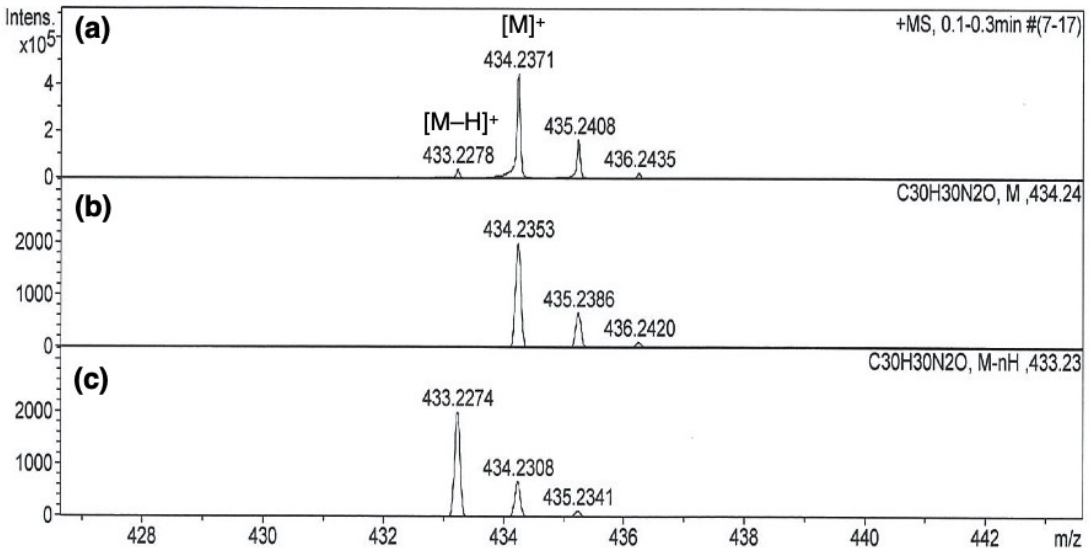

Figure S15. (a) Observed and simulated (b for $[M]^+$, c for $[M–H]^+$) high-resolution APCI mass spectra of **1**.

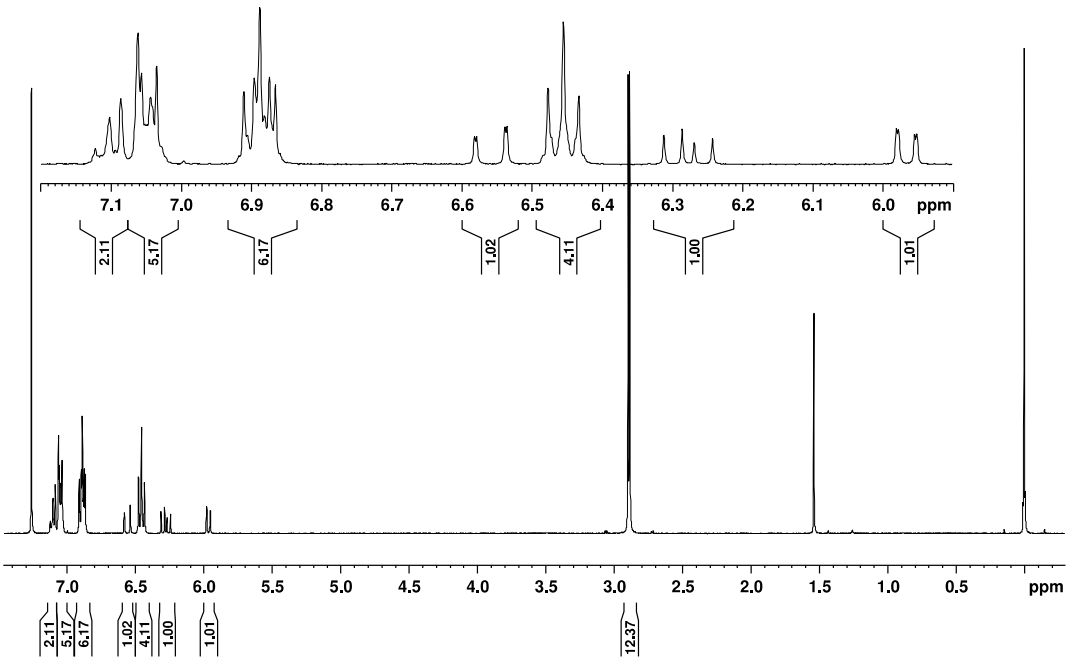

Figure S16. ^{1}H NMR spectrum (400 MHz) of **2** in $CDCl_3$ at 25 °C.

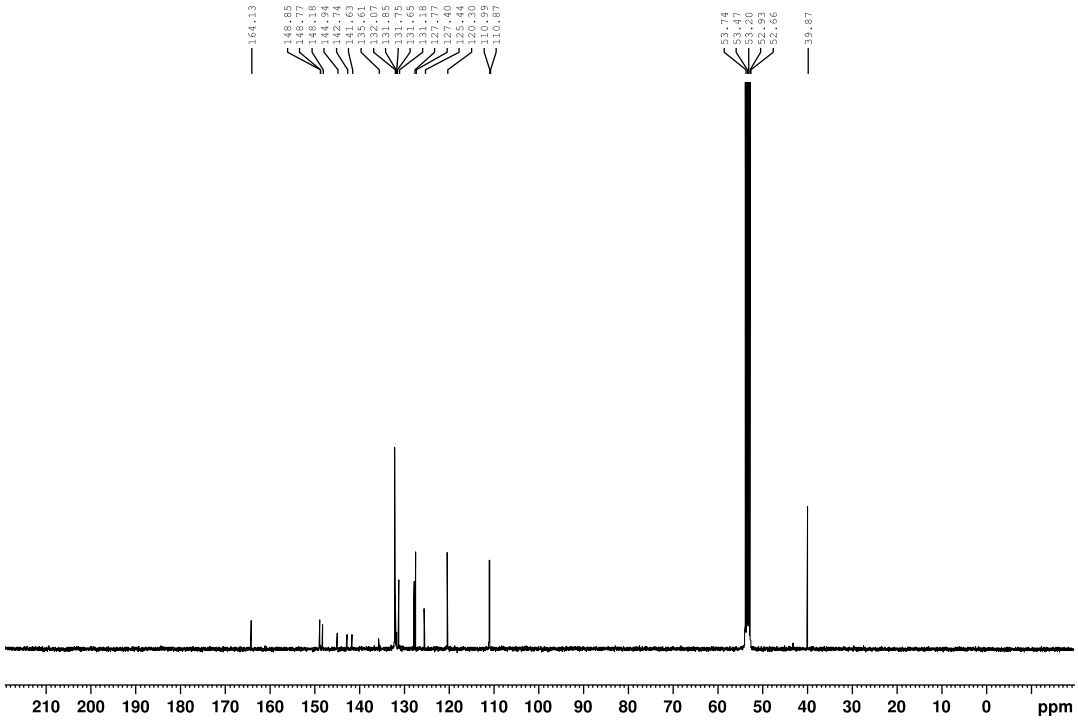

Figure S17. ^{13}C NMR spectrum (100 MHz) of **2** in CD_2Cl_2 at 25 °C.

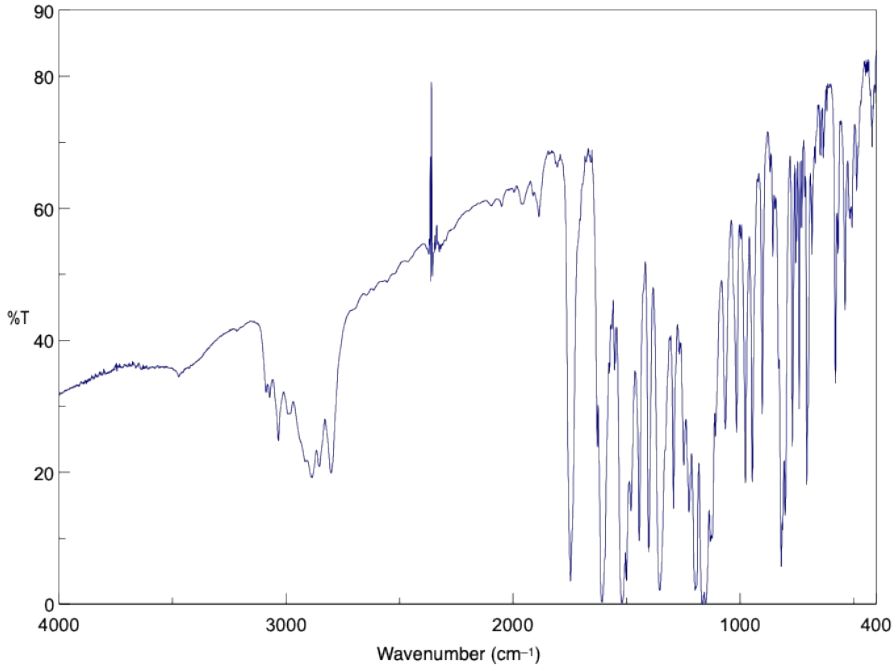

Figure S18. FT-IR spectrum of **2** at 25 °C (KBr).

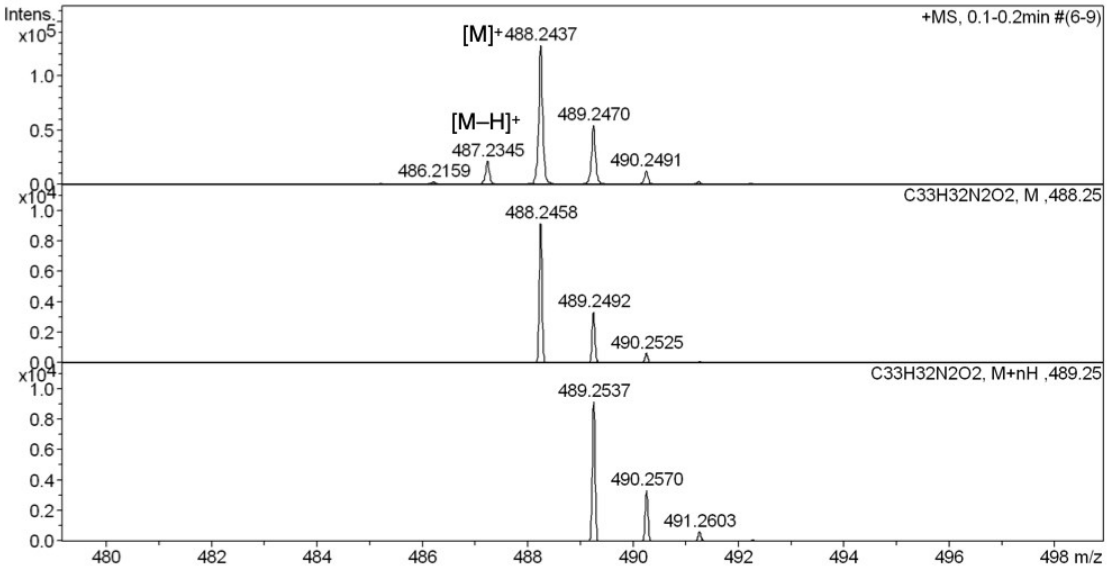

Figure S19. (a) Observed and simulated (b for $[M]^+$, c for $[M+H]^+$) high-resolution APCI mass spectra of **2**.

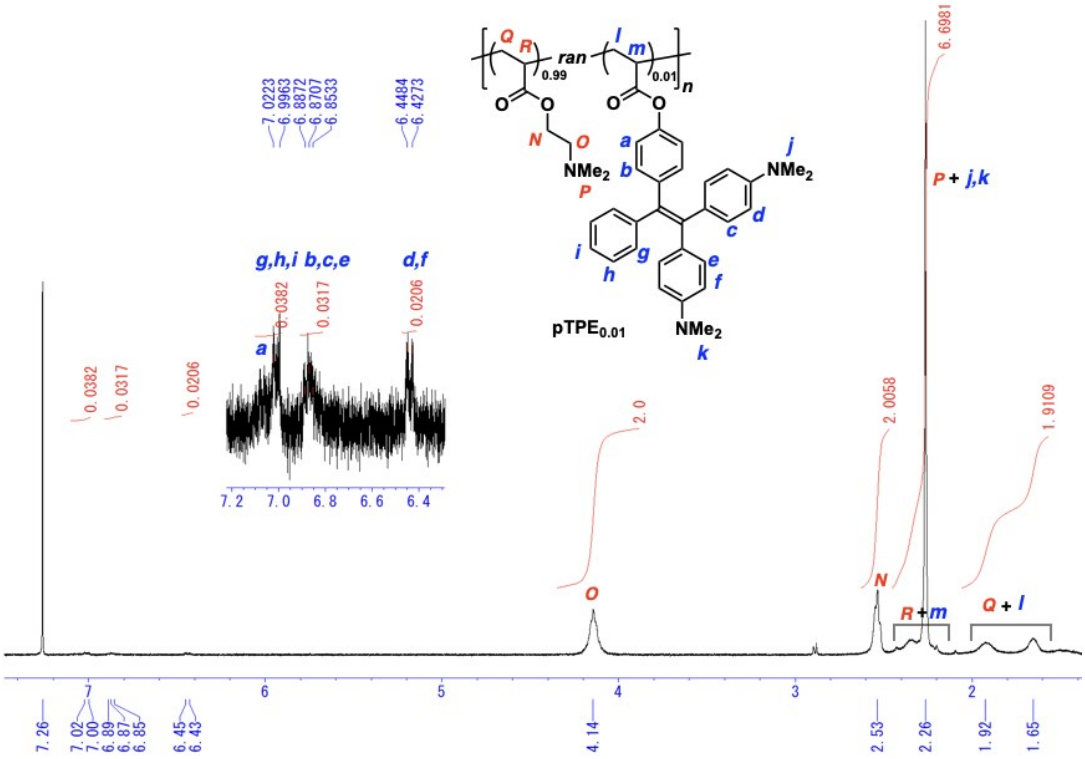

Figure S20. ^{1}H NMR spectrum (400 MHz) of **pTPE$_{0.01}$** in $CDCl_3$ at 25 °C.

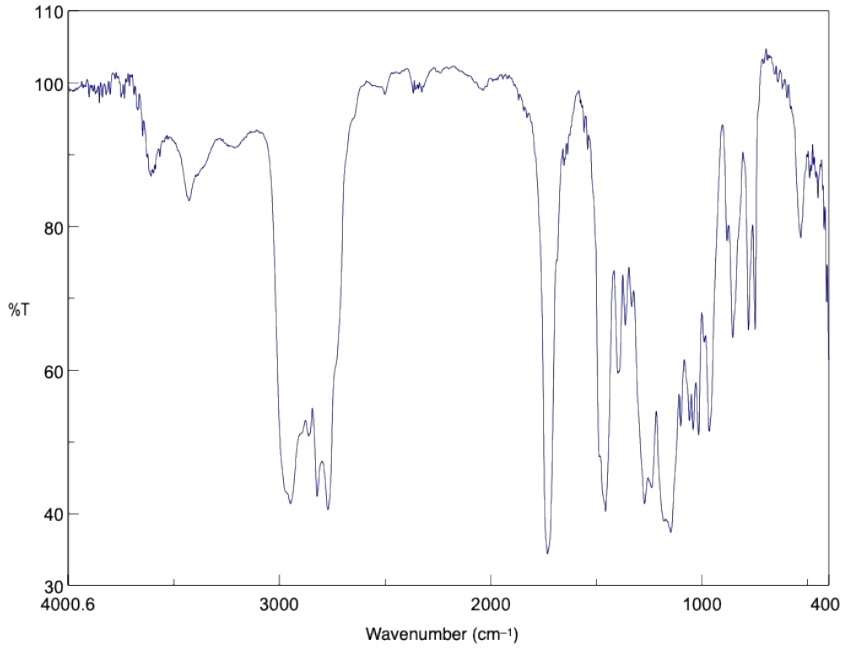

Figure S21. FT-IR spectrum of **pTPE$_{0.01}$** at 25 °C (KBr).

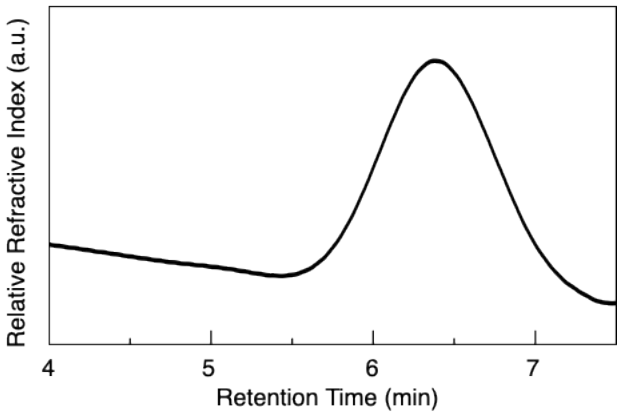

Figure S22. SEC trace of **pTPE$_{0.01}$** (eluent; DMF containing 0.01 M of LiBr).

Reference

[1] S. Ito, T. Sugiyama, N. Toitani, G. Katayama, H. Miyasaka, *J. Phys. Chem. B.* **2007**, *111*, 2365.